Eur. Phys. J. D **22**, 453–459 (2003)
DOI: 10.1140/epjd/e2003-00039-3

THE EUROPEAN PHYSICAL JOURNAL D

A new kind of quantum structure: arrays of cavity solitons induced by quantum fluctuations

I. Rabbiosi[a], A.J. Scroggie[b], and G.-L. Oppo[c]

Department of Physics, University of Strathclyde, 107 Rottenrow, Glasgow G4 ONG, Scotland, UK

Received 20 September 2002 / Received in final form 28 November 2002
Published online 11 February 2003 –

Abstract. Quantum fluctuations of the signal field are shown to induce packed arrays of cavity solitons in a degenerate optical parametric oscillator above threshold in the limit of large pump finesse relative to the signal finesse. The cavity solitons in the array are formed by locked domain walls, and lead to a highly correlated quantum structure. The effect of the quantum fluctuations is non-trivial since the arrays of cavity solitons have a far less stable than other stable solutions and disappear with decreasing pump finesse. The transition from disorder to order due to quantum noise is also discussed.

PACS. 42.65.Sf Dynamics of nonlinear optical systems; optical instabilities, optical chaos and complexity, and optical spatio-temporal dynamics – 42.50.Lc Quantum fluctuations, quantum noise, and quantum jumps – 02.50.Ey Stochastic processes

1 Introduction

Spatial structures in extended nonlinear optical devices can display important quantum features. Quantum images in degenerate optical parametric oscillators (DOPO) show quadrature squeezing in the near field [1,2], and Einstein-Podolsky-Rosen (EPR) correlations in the far field [3]. These effects are due to the generation of entangled photons in the parametric down conversion process within the optical cavity. For a review of these effects see [4,5].

While deterministic spatial structures are commonplace in many branches of science like hydrodynamics, morphogenesis, biological populations, extended chemical reactions etc., the coupling of quantum fluctuations and nonlinear spatial structures is inherent of optics where quantum noise has macroscopic effects even at room temperature. Quantum images are noise driven precursors of the spatial patterns observed above threshold but are induced by quantum fluctuations in photonic devices such as the DOPO, the OPO [6], Kerr cavities [7], and in intracavity second harmonic generation [8]. It is the aim of this paper to present a new kind of spatial structure induced by quantum fluctuations: noisy arrays of cavity solitons formed by locked domain walls. These structures are shown to exist in a DOPO above threshold in the limit of high pump finesse with respect to signal finesse. They differ from other kinds of quantum structure in that they (i) are induced but not sustained by quantum fluctuations, (ii) are not associated with any pattern formation mechanism and (iii) their average size increases with increasing ratio of pump to signal finesse. Arrays of cavity solitons are very weak when compared to other stable solutions such as the single cavity soliton and the homogeneous state and yet such arrays are the asymptotic states selected by the quantum noise.

The paper is organised as follows. In Section 2 we discuss the quantum Langevin model used to describe quantum fluctuations of the pump and signal fields above threshold in a DOPO. In particular we show that in the Wigner representation signal fluctuations dominate in the limit of high pump finesse, and adopt a model recently introduced to describe macroscopic quantum fluctuations in DOPO [10]. Section 3 contains a short discussion on deterministic spatial solutions (including locked domain walls, cavity solitons and spatial chaos) and their stability. The results of the quantum stochastic simulations are presented in Section 4, where the asymptotic arrays of spatial solitons induced by quantum fluctuations are described and characterised in the near and the far fields. Section 5 contains a discussion about noise induced transitions from disordered to ordered spatial structures and about future research directions.

2 Quantum Langevin equations

We consider a $\chi^{(2)}$ material, contained in a single port cavity with plane mirrors, under the action of a pump field

[a] e-mail: ivan@phys.strath.ac.uk
[b] e-mail: andrew@phys.strath.ac.uk
[c] e-mail: gianluca@phys.strath.ac.uk

of frequency 2ω. Degenerate parametric down conversion in the medium generates a signal field at frequency ω. The intracavity pump and signal fields are described by the quantum operators $A_0(x,t)$ and $A_1(x,t)$, respectively, where x is the transverse coordinate. We restrict ourselves here to the one dimensional (1D) DOPO case but many of our results can be immediately generalised to the entire transverse plane.

In the interaction picture the Hamiltonian is given by [2]

$$H = H_f + H_{\rm int} + H_{\rm ext} \tag{1}$$

where

$$H_f = -\hbar \int {\rm d}x\, A_0^\dagger\, (a_0 \partial_{xx}^2) A_0 - \hbar \int {\rm d}x\, A_1^\dagger\, (a_1 \partial_{xx}^2) A_1 \tag{2}$$

includes diffraction,

$$H_{\rm int} = \frac{{\rm i}\hbar g}{2} \int {\rm d}x\, \left(A_0 A_1^{\dagger 2} - A_0^\dagger A_1^2 \right), \tag{3}$$

is the Hamiltonian of the nonlinear interaction, and

$$H_{\rm ext} = {\rm i}\hbar \int {\rm d}x\, \left(E_{\rm in} A_0^\dagger - E_{\rm in}^* A_0 \right), \tag{4}$$

contains the external driving pump. In equation (2) $a_0 = c/(2k_z)$ and $a_1 = 2a_0$ are characteristic diffraction coefficients with c the speed of light and k_z the longitudinal wave vector of the pump wave, while ∂_{xx}^2 is the second partial derivative with respect to space, describing diffraction in the paraxial approximation. Note that we are working at resonance for both the pump and signal field which is the most common operation for realistic cw OPO. Our results, however, can be easily generalised to include detunings from resonance. In equation (3) g is the coupling parameter related to the medium nonlinearity, while in equation (4) $E_{\rm in}$ is the (scaled) plane wave input field amplitude.

The irreversible part of the dynamics is introduced in the Liouvillian terms of the master equation for the density matrix [2]. The master equation is then turned into a set of stochastic differential equations for c-number fields $\alpha_0(x,t)$ and $\alpha_1(x,t)$ corresponding to the operators $A_0(x,t)$ and $A_1(x,t)$, in the Wigner representation [1,2,4]. The procedure introduced in [2,9] by using functional derivatives, has since been repeated for many quantum systems other than the DOPO and we do not repeat it here. The final nonlinear Langevin equations truncated at third order in the Wigner representation and at resonance are [9],

$$\partial_\tau \alpha_0 = -\Gamma \alpha_0 + \Gamma E_{\rm in} - \frac{1}{2}\alpha_1^2 + \frac{\rm i}{2}\partial_{xx}^2 \alpha_0 + \sqrt{\frac{2\Gamma}{n_{\rm th}}}\, \xi_0 \tag{5}$$

$$\partial_\tau \alpha_1 = -\alpha_1 + \alpha_0 \alpha_1^* + {\rm i}\partial_{xx}^2 \alpha_1 + \sqrt{\frac{2}{n_{\rm th}}}\, \xi_1 \tag{6}$$

where

$$\Gamma = \frac{\gamma_0}{\gamma_1} = \frac{T_0}{T_1} = \frac{\mathcal{F}_1}{\mathcal{F}_0} \tag{7}$$

is the ratio of the pump photon decay rate γ_0 (transmittivity T_0) to that of the signal field γ_1 (T_1) and also the ratio of the signal to pump finesse that in the small transmittance limit reduce to $\mathcal{F}_i = \pi/T_i$ with $i = 0, 1$; time has been renormalised *via* $\tau = \gamma_1 t$; all the fields (including $E_{\rm in}$) have been rescaled by $(\gamma_1\sqrt{l_d})/g$; space has been renormalised by $\sqrt{a_1/\gamma_1}$; $n_{\rm th}$ is the number of pump photons necessary to reach the signal generation threshold in the diffraction length l_d, *i.e.*

$$n_{\rm th} = \frac{\gamma_1^2}{g^2}\, l_d = \frac{\gamma_1^2}{g^2}\, \sqrt{a_1/\gamma_1}\,; \tag{8}$$

and finally the variables ξ_0 and ξ_1 are stochastic Gaussian processes with zero average, and correlation,

$$\langle \xi_i(x,\tau)\, \xi_i^*(x',\tau') \rangle = \frac{1}{2}\delta(x-x')\delta(\tau-\tau') \tag{9}$$

with $i = 0, 1$. The noise terms are interpreted as vacuum quantum noise entering through the partially transmitting mirror.

Equations (5, 6) are in a form suitable for the fluctuation-dissipation analysis. One can immediately see that the signal field fluctuates and dissipates at a higher rate than the pump in the limit of small Γ. This is exactly the limit where arrays of cavity solitons induced by quantum fluctuations, as described below, arise. The reduction of the amplitude of the pump fluctuations with respect to the signal fluctuations when $\Gamma \to 0$ is in agreement with two simple observations. The first one is that for small Γ the pump intracavity amplitude is on average much larger than that of the signal and is then less affected by the quantum noise entering through the mirror as well as its associated losses. Second, cavity solitons in the DOPO are due to the locking of domain walls in the signal field so for them to be formed and erased by quantum fluctuations they require a limit where signal fluctuations are dominant.

Before we proceed, we introduce a further normalisation of the fields to recast equations (5, 6) into a more familiar form of the kind introduced in [9]. We renormalise the signal field to $\hat{\alpha}_1 = \alpha_1/\sqrt{2\Gamma}$. After dropping the hat, the Langevin equations are given by:

$$\partial_\tau \alpha_0 = \Gamma \left(-\alpha_0 + E - \alpha_1^2 \right) + \frac{\rm i}{2}\partial_{xx}^2 \alpha_0 + \sqrt{\frac{2\Gamma}{n_{\rm th}}}\, \xi_0 \tag{10}$$

$$\partial_\tau \alpha_1 = -\alpha_1 + \alpha_0 \alpha_1^* + {\rm i}\partial_{xx}^2 \alpha_1 + \sqrt{\frac{1}{n_{\rm th}\Gamma}}\, \xi_1. \tag{11}$$

These equations clearly show that in the limit of small Γ the fluctuations of the pump field lose relevance while those of the signal field increase in amplitude. In this regime of large signal fluctuations and small pump fluctuations, Zambrini *et al.* [10] have shown that the quantum behaviour of the system in the Wigner representation is suitably described by

$$\partial_\tau \mathcal{A}_0 = \Gamma \left(-\mathcal{A}_0 + E - \alpha_1^2 \right) + \frac{\rm i}{2}\partial_{xx}^2 \mathcal{A}_0 \tag{12}$$

$$\partial_\tau \alpha_1 = -\alpha_1 + \mathcal{A}_0 \alpha_1^* + {\rm i}\partial_{xx}^2 \alpha_1 + \sqrt{\frac{1}{n_{th}\Gamma}}\, \xi_1 \tag{13}$$

where $\mathcal{A}_0$ is the "classical" pump field. In equations (12, 13) we have first neglected pump fluctuations since they are unimportant when compared with the fluctuations of α_1^2 and then considered the pump as a classical field [10]. Equations (12, 13) are the quantum stochastic model used in this paper to simulate the effect of quantum fluctuations in a DOPO system above threshold and with high pump cavity finesse. Equations (12, 13) are integrated numerically by using a Milshtein's method as described in [19].

Note that all the results of this paper are presented for the output signal field in the original units which is related to the intracavity field α_1 through the input-output relation

$$\alpha_1^{\rm out} = \sqrt{4\Gamma n_{\rm th}}\ \alpha_1 - \xi_1. \qquad (14)$$

3 Domain walls, cavity solitons and spatial chaos in DOPO

In order to understand the nature of the solutions induced by the quantum fluctuations, we review the properties and the stability of the steady states of the deterministic equations corresponding to the removal of the fluctuations in equation (13). The spatially extended DOPO above threshold is a peculiar spatio-temporal system since it admits an infinite number of stable steady state solutions. In statistical physics this feature is typical of spin-glass systems [11].

The deterministic DOPO admits two stable homogeneous steady state solutions $A_0^s = 1$, $A_{1\pm}^s = \pm\sqrt{E-1}$ and an unstable one $A_0^s = E$, $A_1^s = 0$ above the threshold for signal generation ($E > 1$). It is important to note that there are no modulational instabilities of the homogeneous solutions for any value of E and Γ [12]. The 1D DOPO model admits also domain wall (DW) solutions [13,14] corresponding to heteroclinic trajectories *i.e.* trajectories in the phase space that connect the two stable homogeneous states asymptotically for $x \to \pm\infty$ by passing through the unstable solution $A_1^s = 0$, which defines the core of the defect (Ising wall).

In a DOPO at resonance, DW have oscillatory tails and pairs of DW can lock at fixed incommensurate distances s_j ($j = 0, 1, 2, ...$). They form an entire family of stationary stable solutions. Distances s_j are measured between the centers of two adjacent DW and can be uniquely identified by the number j of oscillations occurring between two DW. For increasing DW distances, the modulus of the largest stability eigenvalue of the corresponding locked state quickly decreases with the order j and eventually DW become independent of each other at large distances [14]. Locked DW correspond to homoclinic (rather than heteroclinic) trajectories in phase space and we speak of localized structures, or cavity solitons (CS), when the locking distance is small [14]. In this case the trajectory originates from one fixed point and returns back to it, remaining substantially far from the opposite equilibrium point. The homoclinic orbits may pass very close to the origin (where both real and imaginary parts of the signal field are equal to zero) but never through it. The real part of A_1, however, must vanish twice and we identify the core of a defect with $\mathrm{Re}(A_1) = 0$. Note that for any generic CS A_1^s, the negative $-A_1^s$ is also a solution.

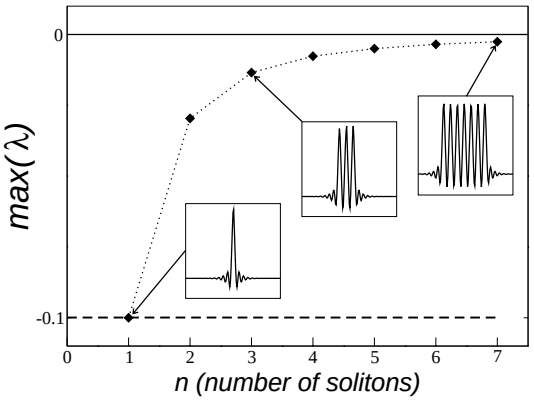

Fig. 1. Largest stability eigenvalue λ for a family of homoclinic solutions corresponding to arrays formed by one to seven cavity solitons.

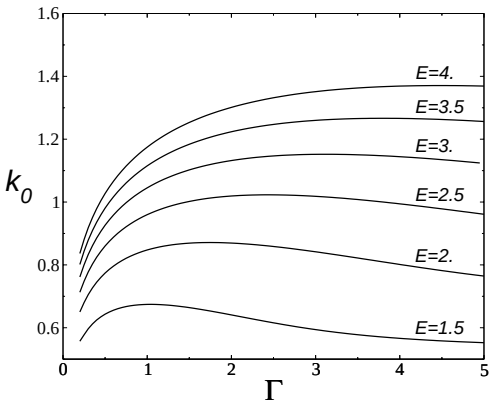

Fig. 2. The wave vector of arrays of cavity solitons k_0 *versus* Γ for several values of the input pump E and no noise.

A second family of stable homoclinic solutions corresponds to arrays of spatial solitons where a number of soliton peaks are found before returning to the initial homogeneous state. In Figure 1 we present the stability of a collection of these homoclinic solutions starting from a single peak and reaching 7 peaks. The largest (negative) stability eigenvalue of the solutions is plotted *versus* the number of soliton peaks in the solution [15]. The steady state solutions and their stability are determined using the numerical methods described in [14,16]. One can easily see from Figure 1 that the solution grows weaker with increasing number of soliton peaks, the single soliton peak being the most stable of all. Periodic arrays of spatial solitons are characterised by the wave vector $k_0 = \pi/s_0$, where s_0 is the size of the single soliton peak. In Figure 2 we present the variation of k_0 with Γ for several values of the input pump E above threshold. For small values of Γ the wave vector k decreases while the soliton peak increases in size.

A generic stationary solution A_1^s consists of a trajectory orbiting around the stable homogeneous states and whose real part vanishes at an even number of points

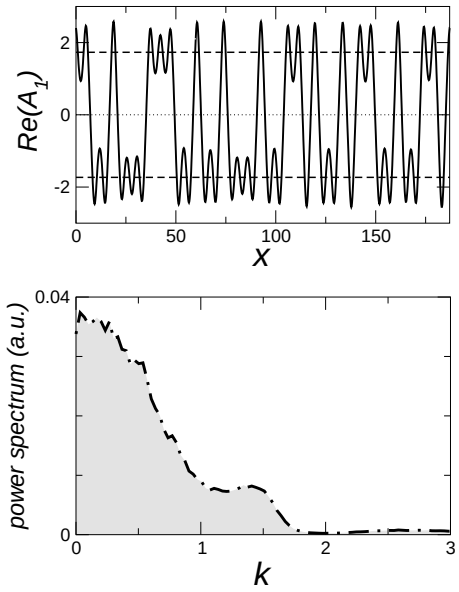

Fig. 3. Typical asymptotic distribution of the real part of the signal field in the absence of fluctuations for $E = 4$ and $\Gamma = 0.2$ (top panel). The spatial power spectrum averaged over many realisations starting from the unstable zero state (bottom panel).

$[x_1, ..., x_{2n}]$ since we are using periodic boundary conditions. The defect cores are located at positions $x_n = x_{n-1} + s_j$, with n, j integers, giving rise to a huge number of possible stable distributions of defects. Note that defect distributions presenting a significant degree of periodicity (where the possible periods are twice the distances s_j), are a very small fraction of the total number. Different final states with arbitrary numbers of defects can be reached by starting from the unstable (zero signal) homogeneous solution with an added random perturbation. The resulting stable 1D structures contain, on average, a wide range of spatial wavelengths giving rise to a continuum background in Fourier space, enhanced by the fact that separations s_j are incommensurate with each other. There is an analogy between this behaviour and temporal chaos, since when $\partial_t = 0$, equations (12, 13) can be considered as a dynamical system with the variable x assuming the role of time. For this reason these aperiodic (disordered) stable structures have been labelled "spatial chaos" by previous authors [17,18]. Figure 3 shows a typical example of a deterministic, stable and disordered solution and its spatial power spectrum. Solutions of this kind are generic in the parameter space (E, Γ).

4 Arrays of cavity solitons induced by quantum fluctuations

In this section we study the effect of quantum fluctuations on the distributions of DW and defects in the signal field. In particular we identify a clear change of behaviour in the spatial spectrum decreasing the ratio Γ between the cavity finesse of pump and signal fields respectively. Figure 4a shows the 1D evolution of the signal field under the action of quantum fluctuations for $\Gamma = 0.02$, $E = 1.5$ and $n_{\rm th} = 1000$. Local fluctuations have been filtered out by introducing a threshold at $\mathrm{Re}(A_1) = 0$ so that the dark (white) regions in Figure 4a represent positive (negative) values of $\mathrm{Re}(A_1)$. Moreover, we eliminate those defects pairs whose separation is less than a definite critical distance since they are doomed to disappear [20]. After a transient whose duration increases exponentially with increasing $n_{\rm th}$, we reach a stationary equilibrium regime where the average number of defects remains constant. This corresponds to a balance between the rates of appearance and disappearance of pairs of DW. We stress that all quantities considered below are evaluated at equilibrium.

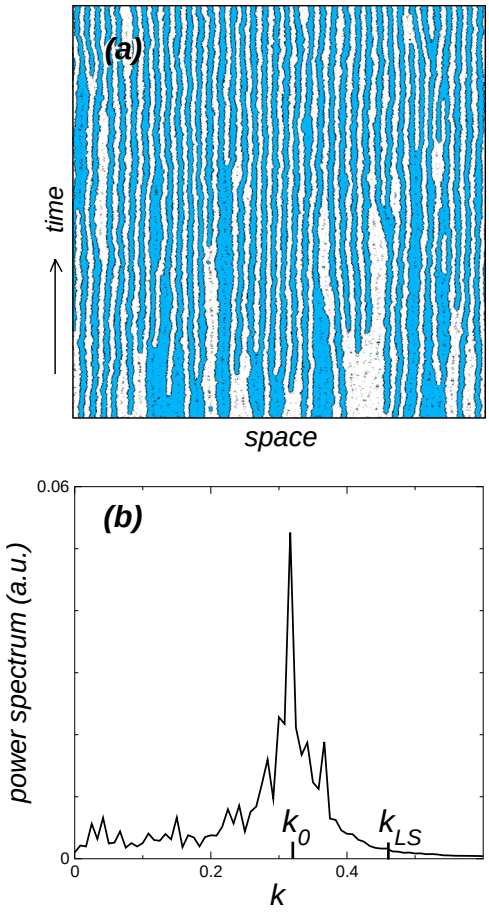

Fig. 4. (a) Temporal evolution driven by quantum fluctuations of the real part of the output signal field for $E = 1.5$ and $\Gamma = 0.02$. Arrays of cavity solitons are clearly visible after the transient has ended. (b) The Fourier spectrum of the spatial auto-correlation function $C[\mathrm{Re}(A_1)]$, averaged over time after the equilibrium state has been reached. k_0 corresponds to the wave vector of arrays of cavity solitons and $k_{\rm LS}$ to the largest eigenvalue of the linear stability analysis of the stable homogeneous solution, away from $k = 0$.

For low Γ, a large number of locked cavity solitons are clearly visible in the near field. They form arrays that

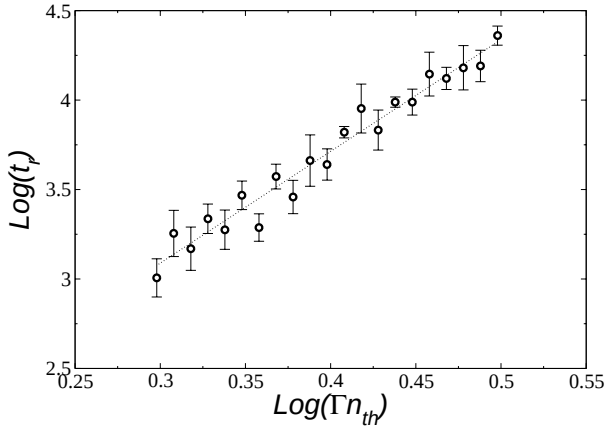

Fig. 5. Duration of the transient t_r before the equilibrium regime is reached *versus* $\Gamma n_{\rm th}$ on a logarithmic scale for $E = 2.6$.

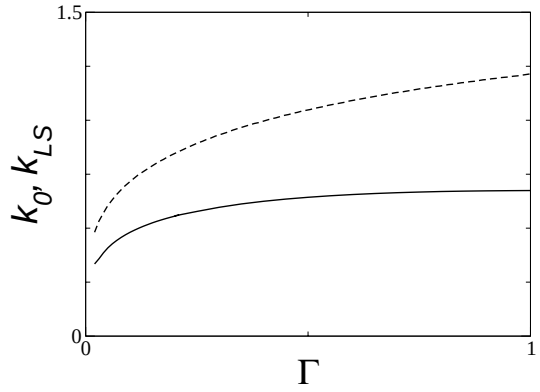

Fig. 6. Wave vectors k_0 (solid line) of the arrays of cavity solitons and k_{LS} (dashed line) corresponding to the largest eigenvalue of the linear stability analysis of the stable homogeneous solution away from $k = 0$ *versus* Γ for $E = 1.5$.

jitter under the action of the fluctuations. The lengths of the arrays are an arbitrary multiple of the soliton size s_0. The average length of the arrays increases with increasing ratio of pump to signal finesse. For example, in Figure 4a this average length is larger than the transverse simulation size. The presence of arrays of cavity solitons is reflected in the far field where a huge peak at k_0 appears. The power spectrum shown in Figure 4b is nothing else than the Fourier transform of the spatial auto-correlation function $C[g(x,t)] = \int_{-\infty}^{+\infty} h(x+x',t)h^*(x',t)\mathrm{d}x'$ averaged over time. In our case $h = \mathrm{Re}(A_1)$. The average size of the arrays of cavity solitons is given by the inverse of the decay rate of the averaged spatial correlation function. A large peak at k_0 in the power spectrum signals the presence of large spatial correlations at distances of the order of s_0.

These arrays should not be confused with patterns above a modulational instability since they are formed by progressive locking of localised structures and not by the instability of a given wave vector. The phenomenon described here is analogous to the noise induced suppression of spatial chaos presented in [20] but is now entirely due to quantum fluctuations. Arrays of cavity solitons in the signal intensity in the limit of small Γ and the corresponding off-axis peak in the far field are a new "quantum structure" in that they are induced by quantum noise after long transients. Note that without the quantum fluctuations the far field is broad band and displays no correlations at any particular wave vector.

One of the main aims of this paper is to show that realistic quantum fluctuations can induce arrays of cavity solitons in a 1D configuration of a DOPO. For this reason Figure 5 shows the duration of the transient before reaching the equilibrium regime against $n_{\rm th}\Gamma$, a parameter that measures the inverse of the fluctuation strength and depends on the pump wavelength, the diffraction in the cavity, the material nonlinearity and the finesse of both cavities. It is important to note that Γ cannot be pushed below say 10^{-3} to maintain the validity of the mean field limit [21] while large values of $n_{\rm th}$ can lead to undesirably long transients. Staying above but close to the threshold of signal generation also helps to achieve optimal balance among the parameters and for this reason we have chosen to work within the range of $1.5 \leq E \leq 3$.

It is important to demonstrate that the quantum structure described here is fundamentally different from the quantum images observed around a modulational instability as described for DOPO in [2,9], for OPO in [6], for Kerr cavities in [7], and for intracavity second harmonic generation in [8]. In all these cases, the quantum image is associated with a noisy precursor of the pattern which forms above a modulational instability. This means that if we switch the noise off after the formation of the quantum image, the far field peak at the critical wave vector k_c of pattern formation above the modulational threshold disappears. In the present case of arrays of cavity solitons, instead, if we remove the noise after the arrays have been induced by the quantum fluctuations, the arrays will survive indefinitely since they are one of many stable stationary-solutions of the system. In this respect it is important to note that our arrays of cavity solitons are induced but *not sustained* by quantum fluctuations. The arrays of solitons described here are also quite different from the periodic sequence of DW with a wave number due to walk-off presented in [22]. Again, the structures observed in [22] are sustained by noise while our arrays of cavity solitons are not. Our noise induced structures are also very different from stochastic distributions observed in [23]. These are nothing else than noise sustained precursors above the signal generation threshold but below a modulational instability of the homogeneous solution obtained at resonance because of the peculiar choice of the diffraction coefficients [24]. The wave number of the stochastic distributions observed in [23] has been obtained through the linear stability of the homogeneous solution and has no relevance to the cavity soliton structures presented here. To elucidate this issue, we display in Figure 6 both wave vectors k_0 of the arrays of cavity solitons, and $k_{\rm LS}$ corresponding to the largest eigenvalue of the linear stability analysis of the stable homogeneous solution away from $k = 0$. These two wave vectors have very different sizes, very different physical origins and are not related to

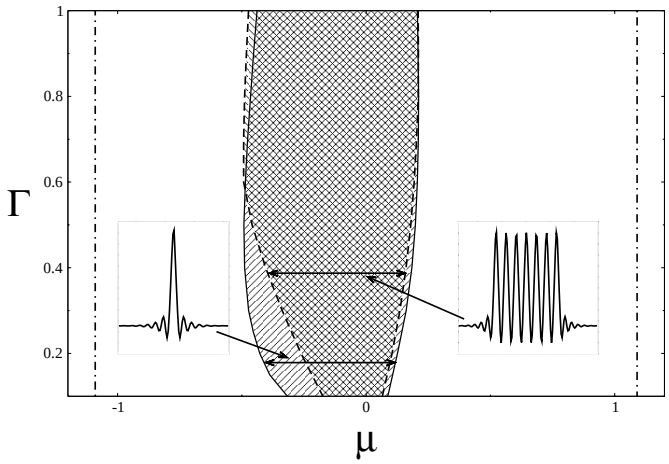

Fig. 7. Existence boundaries of stable multi-defect solutions in the parameter space (μ, Γ) for $E = 3$ when a bias μ is added to (13). Shaded regions represent the existence limits for upward-oriented single peak (right-shaded region enclosed by solid lines) and 7 peak (left-shaded region enclosed by dashed lines) solitonic solutions, as indicated by the arrows. The existence region for the two stable homogeneous states $A^s_{1\pm}$ is within the dotted-dashed vertical lines.

each other through a linear transformation. There is indeed no peak in the spatial Fourier spectrum of Figure 4b corresponding to $k_{\rm LS}$.

The appearance of arrays of cavity solitons induced by quantum fluctuations is nontrivial and is related to the non-potential nature of our model. We note that unlike *e.g.* quartic potential systems, the linear stability of the stationary states does not provide useful information on the relative stability of the solutions. A qualitative criterion to establish the relative stability of the various multi-defects solutions is to look for the loss of their stability when we add a bias to (13), in the form of a constant real term μ, and consider equations (12, 13) without noise. By increasing μ adiabatically we find the critical value at which a given stable stationary state disappears. In Figure 7 we plot in the parameter space (μ, Γ) the existence boundaries of the upward-oriented single-peak (right-shaded region enclosed by solid lines) and seven-peak (left-shaded region enclosed by dashed lines) solitonic solutions, as indicated by the arrows. Note that the existence limits of downward oriented solitonic solutions $(-A^s_1)$ are simply the mirror image with respect to $\mu = 0$ of the diagrams for upward oriented ones (A^s_1). We also note that for low Γ and on increasing $|\mu|$, the first multi-peak solutions to disappear are those with a large number of peaks while the single-peak soliton is the last. Furthermore the stable homogeneous states $A^s_{1\pm}(\mu)$ survive up to very large values of $|\mu|$ and are the last stable states to disappear (dot-dashed vertical lines in Fig. 7).

This heuristic analysis suggests that the most stable states in our system are the two equivalent states $A^s_{1\pm}$. Arrays of cavity solitons in the presence of noise arise as a symmetry-restoring equilibrium state and $\mathrm{Re}(A_1)$ is equally distributed on both sides of $\mathrm{Re}(A_1) = 0$.

Symmetry alone is not enough to explain why quantum fluctuations select regular arrays of cavity solitons since stable homogeneous solutions exist also for large Γ. A simple complementary argument is suggested in [20]. In the limit of small Γ, local oscillations at the tails of the locked DW have large amplitude [14]. Once a single peak cavity soliton is excited by the fluctuations, the probability of exciting another soliton peak in the vicinity of the first one is spatially inhomogeneous due to the presence of the oscillatory tails. In particular fluctuations much smaller than that necessary to excite a single peak soliton from a homogeneous background can excite a new peak in the vicinity of the large amplitude oscillations of the soliton tail. This was determined by finding the unstable single-soliton solution which provides the critical magnitude of such excitations. In the limit of small Γ the critical amplitudes for erasing a soliton peak are larger than those for its excitation as shown in [20], and so the equilibrium density of defects is large. Therefore the average separation distance between defects is small and, since this cannot be smaller than s_0 (the characteristic size of a soliton), arrays of solitons form.

The heuristic argument provided above explains the critical role played by the parameter Γ in the stochastic selection of the final solutions. In particular the condition of small Γ has a twofold relevance; it increases both the role played by the signal noise and the size of the local oscillations of the soliton tails. In agreement with this argument, we observe for increasing Γ that the average size of the arrays of cavity solitons tends to decrease and larger patches of homogeneous solutions progressively appear. This means that the peak in the far field gradually decreases and eventually disappears on increasing Γ. We note however that by increasing Γ the validity of the quantum model (12, 13) becomes questionable since the fluctuations of the pump field cannot be neglected any longer [10]. If we use equations (10, 11) for increasing Γ, we observe arrays of solitons to progressively decrease in size and finally to disappear well before $\Gamma = 1$ leaving the dynamics to be dominated by domain walls performing random walks [20].

5 Discussion and conclusion

We have shown that quantum fluctuations in the signal field can induce arrays of cavity solitons in the output of 1D DOPO. These structures are different from noise sustained quantum images below a modulational instability threshold. Arrays of cavity solitons are in fact stable (yet very unlikely) solutions of the DOPO equations without noise, are not associated with any unstable wave vector, and are induced but not sustained by quantum noise. In particular we have provided important information for their experimental observation. Noise induced arrays of cavity solitons require small Γ, large 1D aspect ratios, and proximity to the signal generation threshold if $n_{\rm th}$ is large.

Noise induced arrays of cavity solitons represent an unusual transition where noise, generally believed to increase

disorder, replaces spatial broad band spectra of the deterministic solutions with highly correlated periodic structures of cavity solitons corresponding to a large peak in the Fourier spectrum. This unusual "disorder to order" transition mediated by noise has been already discussed in [20] where its differences from a stochastic resonance phenomenon [25] have also been discussed.

Our analysis focused on the resonant case to avoid confusion between the emergence of arrays of cavity solitons due to quantum fluctuations and other structures caused by modulational instabilities of homogeneous states. However, we find noise induced arrays of cavity solitons in detuned DOPO whenever the homogeneous solutions $A^s_{1\pm}$ are stable and Γ is small. We are investigating regimes where these noise induced structures arise close to a modulational instability for positive signal detunings or above the threshold of pattern formation for negative detunings. Furthermore it is possible to generalise noise induced arrays of cavity solitons when the homogeneous states $A^s_{1\pm}$ have undergone a modulational instability as happens for positive signal detunings. These results will be presented elsewhere.

We are also working on the characterisation of quantum features in noise induced arrays of cavity solitons. Squeezing properties of the output fields [1,2] and EPR correlations [3] observed in standard quantum images in DOPO may be substantially modified in the case of noise induced arrays of cavity solitons. Their effect on the quantum features associated with the entanglement of twin photons is presently under investigation.

We are also investigating the 2D case which is not a straightforward generalisation of the 1D case as, for example, in standard quantum images. In 2D, curvature effects strongly affect the position and the interaction of cavity solitons [14]. We expect noise to be less efficient in modifying the overall output characteristics of the signal field in 2D than in 1D. These results are however important in determining the best experimental DOPO configuration for the observation of the formation and correlations of our new quantum structure formed by locked cavity solitons.

We thank Alessandra Gatti, John Jeffers and Roberta Zambrini for useful discussions. G-LO thanks SGI for financial support. We acknowledge support from EPSRC (GR/M19727, GR/M31880, GR/R04096 but unfortunately not from GR/S21496) the EC (contract IST-2000-26019 QUANTIM) and SHEFC (grants VISION and VIDEOS). One of us (G-LO) would like to take advantage of this occasion to thank the EC and all partners and participants to the TMR network QSTRUCT which ended in 2001. Your constant support and great enthusiasm have made the coordinating job very easy and enjoyable.

References

1. A. Gatti, L.A. Lugiato, Phys. Rev. A **52**, 1675 (1995)
2. A. Gatti, H. Wiedemann, L.A. Lugiato, I. Marzoli, G.-L. Oppo, S.M. Barnett, Phys. Rev. A **56**, 877 (1997)
3. I. Marzoli, A. Gatti, L.A. Lugiato, Phys. Rev. Lett. **78**, 2092 (1997)
4. L.A. Lugiato, M. Brambilla, A. Gatti, Adv. At. Mol. Opt. Phys. **40**, 229 (1999)
5. M. Kolobov, Rev. Mod. Phys. **71**, 1539 (1999)
6. C. Szwaj, G.-L. Oppo, A. Gatti, L.A. Lugiato, Eur. Phys. J. D **10**, 433 (2000)
7. R. Zambrini, M. Hoyuelos, A. Gatti, P. Colet, L.A. Lugiato, M. San Miguel, Phys. Rev. A **62**, 063801 (2000)
8. M. Bache, P. Scotto, R. Zambrini, M. San Miguel, M. Saffman, Phys. Rev. A **66**, 013809 (2002)
9. A. Gatti, L.A. Lugiato, G.-L. Oppo, R. Martin, P. Di Trapani, A. Berzankis, Opt. Express **1**, 21 (1997)
10. R. Zambrini, S.M. Barnett, P. Colet, M. San Miguel, Phys. Rev. A **65**, 023813 (2002); see also erratum by the same authors and M. San Miguel, *ibid.* **65**, 049901 (2002)
11. M. Mezard, G. Parisi, M.A. Virasoro, *Spin Glass Theory and Beyond* (Word Scientific, Singapore, 1986)
12. G.-L. Oppo, A.J. Scroggie, S. Sinclair, M. Brambilla, J. Mod. Opt. **47**, 2005 (2000)
13. S. Trillo, M. Halterman, A. Shepard, Opt. Lett. **22**, 970 (1997)
14. G.-L. Oppo, A.J. Scroggie, W.J. Firth, J. Opt. B **1**, 133 (1999); Phys. Rev. E **63**, 66209 (2001)
15. All these solutions are obviously invariant by translation. This means that the zero eigenvalue corresponding to translational motion has been removed from Figure 1
16. J. McSloy, W.J. Firth, G.K. Harkness, G.-L. Oppo, Phys. Rev. E **66**, 046606 (2002)
17. P. Coullet, C. Elphick, D. Repaux, Phys. Rev. Lett. **58**, 431 (1987)
18. M.C. Cross, P.C. Hohenberg, Rev. Mod. Phys. **65**, 851 (1993)
19. M. San Miguel, R. Toral, *Stochastic Effects in Nonlinear Systems*, Proc. IEEE **85**, 1 (1997)
20. I. Rabbiosi, A.J. Scroggie, G.-L. Oppo, Phys. Rev. Lett. **89**, 254102 (2002)
21. The mean field limit has been obtained as a first order expansion in the transmittivity of the cavity mirrors. By reducing Γ below say 10^{-3} a new perturbation expansion is necessary to include higher order terms. Note also that the limit of $\Gamma \to 0$ is singular even in the absence of noise and diffraction
22. M. Santagiustina, P. Colet, M. San Miguel, D. Walgraef, Opt. Lett. **23**, 1167 (1998)
23. K. Staliunas, V.J. Sanchez-Morcillo, Opt. Commun. **177**, 389 (2000)
24. We note that the mechanism of noisy precursor in [23] is the same as that described for quantum images in DOPO, OPO and Kerr media
25. L. Gammaitoni, P. Hängi, P. Jung, F. Marchesoni, Rev. Mod. Phys. **70**, 223 (1998)